Separating the coherent and incoherent effects in optical correlation experiments on semiconductors and other saturable absorbers

A. F. Bello, D. J. Erskine, and H. B. Radousky
Lawrence Livermore National Laboratory, Livermore, California 94551

(Received 14 June 1995; accepted for publication 26 October 1995)

In some pump–probe optical correlation experiments, the measured signal versus delay between pulses generally consists of two components: the convolution of the pulse autocorrelation with the sample impulse response, and a coherent artifact. The latter can obscure the first component near zero delay where fast time scale processes will be manifest. We present a mathematical description of the relative shapes and sizes of the two components, so that a fitting process can separate them. This can yield both the dephasing and relaxation times of saturable absorbers such as semiconductors. The method is particularly appropriate when the orientational dephasing and relaxation times are of the same time scale as the laser pulse width. © *1996 American Institute of Physics.* [S0034-6748(96)00702-3]

I. INTRODUCTION

With the advent of femtosecond pulse lasers, researchers are now able to investigate the femtosecond scale dynamics of a variety of materials using short pulse correlation techniques. Suitable samples for transmission experiments are any materials which exhibit saturable absorption. Technologically significant materials of particular interest are semiconductors, such as GaAs, light emitting polymers such as PPV (poly-phenylene-vinylene), or biological materials, such as rhodopsin. The ultrashort time scale behavior of the carrier dynamics is incompletely understood, yet relevant to the design of fast optoelectronic devices such as switches and detectors. Other saturable absorbers, such as dye molecules, can also be studied for their ultrafast intramolecular dynamics.

A basic and widespread short pulse correlation technique is the ''pump–probe.'' The sample is irradiated by two pulses separated by a known delay τ. The integrated transmission of one of the pulses is recorded versus τ, averaged over many repetitions. Ideally, the record produced is a convolution of the material impulse response with the pulse autocorrelation function (AC). Since the latter can be independently measured, a deconvolution process can extract the material impulse response from the experimental record. In order to measure the transmission of only one of the pulses, the pulses may be distinguished by wavelength, angle of incidence, or polarization.

However, in many cases it is impractical to use different wavelengths. And even though the two pulses are distinguished by angle or polarization, they may interact through the material properties to contribute a portion to the transmission correlation record called the coherent artifact (CA). The CA complicates the correlation data near zero delay (having a width not wider than the AC). The confusing effect of the CA has led some investigators to completely forgo the data close to zero delay.[1] This is acceptable when the correlation record is much wider than the CA or AC. However, for fast relaxation processes, the correlation record will have a shape decaying not significantly wider than the CA or AC. In this case the CA cannot be ignored.

The purpose of this report is to present a mathematical framework describing all the correlation components, including the CA, so that the incoherent and coherent components can be separated. Fitting the incoherent components yields the population relaxation time. Fitting the CA component will yield the orientational (dephasing) relaxation time. The physics of the latter is interesting in of itself. Thus, beyond being a nuisance to measuring the population relaxation, the CA can yield significant information of its own. The terminology we use assumes a transmission experiment and generic saturable absorber, however, the model should also apply qualitatively to reflection correlation experiments.

Although the asymmetric pump–probe configuration is the most widely used correlation configuration, we prefer a symmetric correlation technique. That is, there is no attempt to distinguish the pulses. The pulses are collinear, identical in wavelength, of equal intensities, and the transmission of the sum of both pulses is measured versus τ. Their relative polarization may be parallel ($\|$) or orthogonal ($\perp$). This optical correlation technique[2] has been used to measure semiconductor carrier relaxation times[3–9] and the intramolecular dynamics of dye molecules.[10,11] The record produced is called a transmission correlation peak (TCP).

This symmetrical technique excels at measuring relaxation times which are as short or shorter than the pulse AC. This is because the symmetry causes the slow relaxation components to form an almost level background on which the faster components manifest themselves as a peak. The measured width of the peak does not depend on measuring the $\tau=0$ position, which is problematic in the asymmetric (pump–probe) technique. Accurate width measurement is necessary to determine relaxation components faster than the pulse width.

Previous work[12–16] on coherence effects in ultrafast phenomena associated with photoexcited carriers have progressively become complex. Some theories[12–14] have included many-body Coulomb interaction, the semiconductor Bloch equations, or non-Markovian (memory effects) behavior[16] on a fundamental level. However, these are complex numerical calculations requiring large computing power. We use an empirical approach that describes the behavior in terms of a

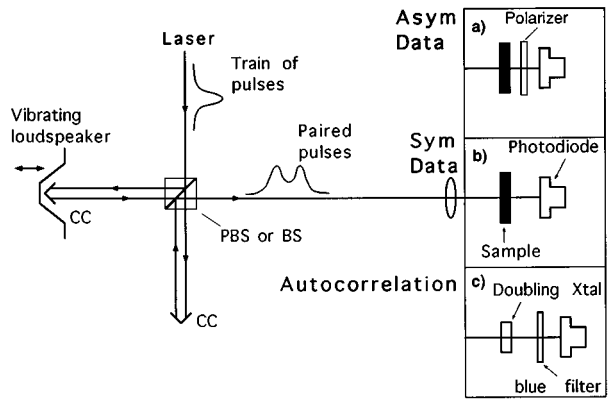

FIG. 1. Experimental setup for obtaining sample correlation peaks: (a) asymmetric: ${}^{\perp}s(\tau)$; (b) symmetric: ${}^{\perp}\mathrm{tcp}(\tau)$ and ${}^{\parallel}\mathrm{tcp}(\tau)$; or (c) pulse autocorrelation: $\mathrm{AC}(\tau)$. The laser produces a train of subpicosecond pulses with period ~10 ns. The interferometer creates two echos separated by a delay τ, collinear and of equal intensity. Relative polarizations can be $\parallel$ or $\perp$ by use of normal (BS) or polarizing beamsplitter (PBS). The delay is scanned by a corner cube (CC) on a vibrating loudspeaker. The photodetector detects time averaged transmitted intensity. Its output vs τ is recorded by digital oscilloscope synchronized to speaker. The asymmetric correlation $s(\tau)$ is measurable only for orthogonal polarizations, when the polarizer behind the sample blocks one transmitted pulse. The blue filter represents any filter which passes doubled laser light while rejecting laser fundamental.

dephasing time T_θ, and a population impulse response $G(t)$ which can be further parametrized in terms of a sum of discrete relaxation times T_i. We use the formalism of Refs. 4 and 17, which uses a density matrix theory adapted to semiconductors.

II. OPTICAL SETUP

Figure 1 describes the experimental arrangement for measuring the four kinds of experimental records versus delay τ used in our analysis: the symmetrical transmission correlation peak in the orthogonal and parallel modes [${}^{\perp}\mathrm{TCP}(\tau)$, ${}^{\parallel}\mathrm{TCP}(\tau)$], the asymmetrical transmission correlation peak [${}^{\perp}s(\tau)$], and the pulse autocorrelation [$\mathrm{AC}(\tau)$]. The details of the laser system and sample are not important for the method we are presenting, except that the repetition period of the laser train (P) must be longer than the longest relaxation time to be studied. This is satisfied for GaAs and dye molecules, where the slowest relaxation times are of the order of a few nanoseconds and the repetition period of our laser is ~10 ns.

The TCP is measured in the $\parallel$ and $\perp$ polarization modes by use of either a polarizing or nonpolarizing beamsplitter. After the symmetric data have been taken in the perpendicular polarization mode [${}^{\perp}\mathrm{TCP}(\tau)$ and Fig. 1(b)], a polarizer is inserted after the sample to block one pulse from the detector. This achieves the asymmetric configuration [${}^{\perp}s(\tau)$ and Fig. 1(a)]. Then by swapping out the sample for a doubling crystal, the pulse autocorrelation $\mathrm{AC}(\tau)$ is measured [Fig. 1(c)].

In all cases the photodetector has a response time much slower than the repetition period of the laser pulse train so that the transmitted intensity is time averaged. The delay τ between pulses is scanned by a corner cube retroreflector mounted on a vibrating loudspeaker. Digitizing electronics record the photodetector output versus time, averaged over many loudspeaker oscillations, and synchronized to speaker position. Subsequent processing converts the horizontal record axis from time to pulse delay.

Using the four experimental records, a fit is made to the model presented below, with independent parameters T_θ and function $G(t)$. The model requires knowledge of a set of coefficients Y_{ij} and Y_{ijkl} which describe the symmetry properties of the saturable absorption process in the sample.[4,17] These coefficients can depend on the semiconductor band structure at the wavelength being probed.[4] We presume that these Y values are known.

III. THEORY

We use the formalism of Refs. 4 and 17, where the density-matrix equations are solved for a three-level system consisting of two levels and a reservoir, describing saturable absorption of carriers interacting with the electric field of the incident beam. The interaction is manifested in the third-order polarization, which describes the change in transmitted intensity. Let the incident field be described by

$$E(t)=\exp(i\omega t)\sum_j E_j(t)\hat{e}_j, \tag{1}$$

where $E_j(t)$ is the envelope of the component having a polarization direction $\hat{e}_j$, and index j is one of two polarization directions $\hat{x}$ or $\hat{y}$, and ω is the carrier frequency underneath the envelope. The relevant component of the third-order nonlinear polarization is then[17]

$$\mathbf{P}^{(3)}(t)\propto i\,\exp(i\omega t)\sum_{ijkl}\hat{e}_i E_j(t)\int_0^\infty dw A_{ijkl}(w)E_k^*(t-w)E_l(t-w) \tag{2}$$

with $A_{ijkl}(t)$ the impulse response of the third-order susceptibility of the system to a particular combination of electric field polarizations. The indices i, j, k, l can represent either the $\hat{x}$ or $\hat{y}$ direction. According to Ref. 17,

$$A_{ijkl}(t)=\{Y_{ij}Y_{kl}[1-\exp(-t/T_\theta)]+Y_{ijkl}\exp(-t/T_\theta)\}G(t), \tag{3}$$

where $G(t)$ is the impulse response of the population of the photoexcited state. Generally, $G(t)$ consists of several components having different relaxation rates. For example in semiconductors, carriers leave their initially photoexcited states on a femtosecond time scale. A thermal distribution is formed which cools on a femto-[18] or picosecond time scale. Other processes, such as carriers returning from outer valleys where they were initially scattered, may contribute picosecond relaxations. These can affect the transmission with negative polarity, such as observed in GaAs.[6] That is, after the femtosecond scale decrease, the transmission may increase on a picosecond scale. The longest decay is on a nanosecond scale, when the carriers make band to band recombination. For a dye molecule, there can also be simultaneous relaxation components on femtosecond, picosecond, and nanosecond time scales.

TABLE I. Effective Y values for the 2.02 eV transition in GaAs (Ref. 4) and for any wavelength in a dye molecule using a simple model (Ref. 17).

	$(Y_{xx})^2$	Y_{xxxx}	Y_{xxyy}	Y_{xyyx}
GaAs at 2.02 eV	0.84	0.092	0.073	0.060
Dye	1/9	1/5	1/15	1/15

Later, we will model $G(t)$ as a sum of exponential decays to achieve analytical expressions for the Gaussian pulse example. However, this is not required if the correlations are computed numerically. In the figures, for clarity we will show only the fast and slow relaxation components, not any intermediate components. Our typical pulse widths are ~100 fs. Consider the fast relaxation times to be several times shorter than this, the medium times to be 1–5 times the pulse width, and the slow times to be very much longer than the pulse width, but less than the pulse train period P (~10 ns).

T_θ is the dephasing or orientational relaxation time and describes the decay of an anisotropic momentum distribution of carriers to an isotropic distribution. For example, transitions from the GaAs heavy-hole band initially result in a photoexcited population of distribution $\sin^2(\theta)$, where θ is the angle between the carrier wave vector and the polarization of the light.

Y_{ij} and Y_{ijkl} are coefficients derived from the projection integrals of the transition-matrix elements which describe the symmetry of the saturable-absorption process.[17] The nonzero values for an isotropic or cubically symmetric semiconductor such as GaAs obey the relations

$$Y_{xx}=Y_{yy}; \quad Y_{xxyy}=Y_{yyxx}; \quad Y_{xyyx}=Y_{yxxy}; \quad Y_{xxxx}=Y_{yyyy}. \tag{4}$$

These may not hold for an anisotropic sample. For a simple molecular model of a dye we also have $Y_{xxyy}=Y_{xyyx}$.

The calculation of these relations for GaAs and AlGaAs is discussed in detail in Ref. 4 and for dye molecules in Ref. 17. The reader will need to calculate these values for the particular semiconductor and transition energy being probed. For purposes of example, we list GaAs values calculated for 2.02 eV (Table I). These are net values, summed over contributions from the heavy-hole, light-hole, and split-off bands weighted by the density of states squared.

The Y values for dye (Table I) using a simple molecular model are derived[17] from general symmetry principles and do not depend on molecule species or transition energy.

The interaction of the applied field with the third-order polarization leads to an induced change in transmitted intensity[19]

$$\Delta I \propto \mathrm{Re}\left[\mathbf{E}^*(t)\cdot\frac{d\mathbf{P}^{(3)}(t)}{dt}\right] \propto \mathrm{Im}[\mathbf{E}^*(t)\cdot\mathbf{P}^{(3)}(t)]. \tag{5}$$

While the measured signal $\mathrm{TCP}(\tau)$ is the total intensity, the calculated signal is only the portion $\Delta\mathrm{TCP}(\tau)$ due to saturable absorption, above the normal (nonsaturable) transmission component. If the pulse train period is sufficiently long then we can express the time average $\Delta\mathrm{TCP}(\tau)\propto\int_{-\infty}^{\infty}dt\Delta I$, so we have

$$\Delta\mathrm{TCP}(\tau)\propto\mathrm{Re}\sum_{ijkl}\int_0^\infty dw A_{ijkl}(w)\int_{-\infty}^{\infty}dt E_i^*(t)E_j(t) \times E_k^*(t-w)E_l(t-w). \tag{6}$$

The applied $\mathbf{E}(t)$ consists of a pair of collinear pulses having the same envelope $E_a(t)$, separated by a delay τ. In the $\perp$ polarization case E_x and E_y in Eq. (1) will be

$$E_x(t)=E_a(t), \quad E_y(t)=E_a(t+\tau)\exp(i\omega\tau) \tag{7}$$

and in the parallel case

$$E_x(t)=E_a(t)+E_a(t+\tau)\exp(i\omega\tau), \quad E_y(t)=0. \tag{8}$$

To find $\Delta\mathrm{TCP}(\tau)$, we substitute Eq. (7) or (8) into Eq. (6) and sum the eight nonzero permutations of A_{ijkl}. These can be reorganized into a sum of asymmetrical terms and their reflections,

$$\Delta\mathrm{TCP}(\tau)=\Delta S(\tau)+\Delta S(-\tau), \tag{9}$$

$$\Delta S(\tau)=s_{\mathrm{in}}(\tau)+s_{\mathrm{ca}}(\tau)+\mathrm{osc}+\mathrm{DI}. \tag{10}$$

$\Delta S(\tau)$ is the asymmetrical correlation peak corresponding to the transmission of only one of the two pulses. $\Delta S(\tau)$ consists of four parts, which for the $\perp$ case are

$$^{\perp}\mathrm{DI}=\int_{-\infty}^{\infty}dt\int_0^\infty dw A_{xxxx}(w)|E_a(t)|^2|E_a(t-w)|^2, \tag{11}$$

$$\mathrm{osc}=\mathrm{Re}\,\exp(i2\omega\tau)\int_{-\infty}^{\infty}dt\int_0^\infty dw A_{yxyx}(w)E_a^*(t+\tau) \times E_a(t)E_a^*(t-w+\tau)E_a(t-w), \tag{12}$$

$$^{\perp}s_{\mathrm{in}}(\tau)=\int_0^\infty dw A_{xxyy}(w)\mathrm{AC}(\tau-w), \tag{13}$$

$$^{\perp}s_{\mathrm{ca}}(\tau)=\int_0^\infty dw A_{xyyx}(w)\xi(w,\tau), \tag{14}$$

where $\mathrm{AC}(\tau)$ is the pulse autocorrelation and $\xi(w,\tau)$ is a coherence correlation

$$\mathrm{AC}(\tau)=\int_{-\infty}^{\infty}dt|E_a(t)|^2|E_a(t-\tau)|^2, \tag{15}$$

$$\xi(w,\tau)=\mathrm{Re}\int_{-\infty}^{\infty}dt E_a^*(t)E_a(t+\tau)E_a^*(t+\tau-w) \times E_a(t-w). \tag{16}$$

The analogous expressions for the $\parallel$ case are obtained from Eqs. (11) to (14) by using A_{xxxx} throughout, in place of A_{xxyy}, A_{xyxy}, etc. Thus,

$$^{\parallel}\mathrm{DI}=^{\perp}\mathrm{DI}, \tag{17}$$

$$^{\parallel}s_{\mathrm{in}}(\tau)=\int_0^\infty dw A_{xxxx}(w)\mathrm{AC}(\tau-w), \tag{18}$$

$$^{\parallel}s_{ca}(\tau)=\int_0^{\infty} dw A_{xxxx}(w)\xi(w,\tau). \tag{19}$$

DI is the delay independent component, which is not of interest, since it cannot be experimentally separated from the normal transmitted intensity. The oscillatory term (osc) is ignored for our purposes, since we scan our delay fast enough that this averages to zero by the photodetecting electronics. (However, it contains some information about the pulse shape.) The components of interest to us are $s_{in}(\tau)$ and $s_{ca}(\tau)$, the incoherent and coherent contributions, respectively.

A. Measured form of data

Our method requires measuring the four quantities $^{\perp}\mathrm{TCP}(\tau)$, $^{\parallel}\mathrm{TCP}(\tau)$, $^{\perp}S(\tau)$, and the pulse autocorrelation $\mathrm{AC}(\tau)$, using different versions of the optical setup [Figs. 1(a)–1(c)]. We are interested in the delay dependent portions, defined as $\mathrm{tcp}(\tau)$ and $s(\tau)$, respectively. (The oscillatory terms are ignored.) These are related to the above calculated terms by

$$s(\tau)=s_{in}(\tau)+s_{ca}(\tau). \tag{20}$$

For every asymmetrical component there is a symmetrical counterpart:

$$\mathrm{tcp}(\tau)=s(\tau)+s(-\tau), \tag{21}$$

$$\mathrm{tcp}(\tau)=\mathrm{tcp}_{in}(\tau)+\mathrm{tcp}_{ca}(\tau). \tag{22}$$

The components $\mathrm{tcp}(\tau)$ and $s(\tau)$ rest above a baseline intensity $\mathrm{TCP}(\infty)$ or $S(\infty)$ which consists of the normally transmitted intensity and DI components,

$$S(\tau)=\mathrm{normal}+\Delta S(\tau), \tag{23}$$

$$\Delta S(\tau)=s(\tau)+\mathrm{DI} \tag{24}$$

and analogously for $\mathrm{TCP}(\tau)$, $\Delta\mathrm{TCP}(\tau)$, and $\mathrm{tcp}(\tau)$. These definitions are illustrated in Figs. 2 and 3. The baseline $\mathrm{tcp}(\infty)=0$ is ideally measured at $\mathrm{TCP}(\infty)$. However, the maximum delay we can attain is the pulse train period P. We assume that P is much longer than the slowest relaxation component so that

$$\mathrm{tcp}(P)\approx\mathrm{tcp}(\infty)=0, \quad s(P)\approx s(\infty)=0. \tag{25}$$

This assumption is met for GaAs and most dye molecules, since $P\sim 10$ ns, and the slowest relaxation components are band to band transitions, which take several ns in GaAs and dye molecules. In the figures and in this text, we will often use the symbol ∞ to mean P.

Because of the pulse train repetition, negative delays beyond the pulse width for $^{\perp}s(\tau)$ are equivalent to positive delays of the order of P (Fig. 3). Thus the baseline is determined from the height ($^{\perp}\Lambda$) of the shoulder in the shape of $^{\perp}s(\tau)$. This immediately gives us the $^{\perp}\mathrm{tcp}(\infty)$ baseline since it shares the same shoulder height. The $^{\parallel}$tcp shoulder height ($^{\parallel}\Lambda$) is related to $^{\perp}\Lambda$ considering the effect of T_θ and Y values. For semiconductors, $^{\parallel}\Lambda \cong {}^{\perp}\Lambda$. For dye molecules $^{\parallel}\Lambda \cong {}^{\perp}\Lambda\ (Y_{xxxx}/Y_{xxyy})$. This can be seen more easily in the Gaussian pulse example discussed later.

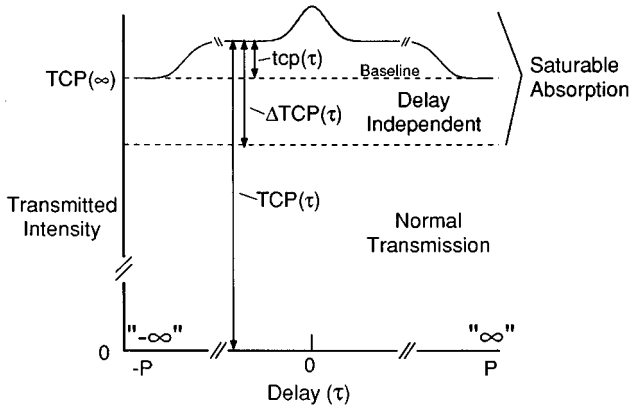

FIG. 2. Definitions of TCP, ΔTCP, and tcp. The definitions $S(\tau)$, $\Delta S(\tau)$, and $s(\tau)$ are corresponding, in asymmetric form. The absolute transmitted intensity vs delay is $\mathrm{TCP}(\tau)$. The portion due to saturable absorption is $\Delta\mathrm{TCP}(\tau)$, and the delay dependent portion is $\mathrm{tcp}(\tau)$. The baseline of $\mathrm{tcp}(\tau)$ is at $\mathrm{tcp}(\infty)$ or $\mathrm{TCP}(\infty)$. The vertical extent of the normal transmission component is greatly reduced for clarity, since $\mathrm{tcp}(\tau)$ is not usually more than a few percent high. The longest delay attainable is the repetition period (P) of the laser train, which is assumed longer than any relaxation time being studied so that $\mathrm{tcp}(P)\cong\mathrm{tcp}(\infty)=0$. For analysis, data are normalized so that $\mathrm{TCP}(\infty)=1$ and $S(\infty)=0.5$.

The experimental data must be normalized so that $\mathrm{TCP}(\infty)=1$ and $S(\infty)=0.5$. Furthermore, the calculated expressions for the $\mathrm{tcp}(\tau)$ and $s(\tau)$ components assumed equal pulse intensities between the two arms. Unequal intensities will not change the horizontal shape of the correlations, only their heights. Their heights are proportional to I_1I_2, where I_1 and I_2 are the intensities from the two arms. If the intensities are different when changing between $\parallel$ and $\perp$ configurations, then one should normalize the heights of $\mathrm{tcp}(\tau)$ and $s(\tau)$, [not $\mathrm{TCP}(\tau)$ and $S(\tau)$], by dividing by I_1I_2.

B. General properties

Let us discuss some general properties before modeling the pulse envelope by a specific shape. In the analysis we will compare components heights measured at $\tau=0$. We note from inspection of Eqs. (18) and (19) that

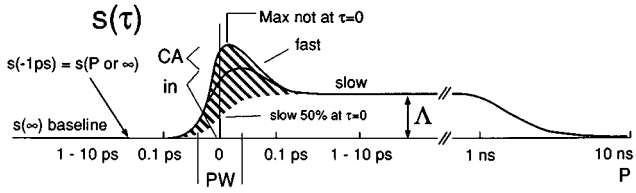

FIG. 3. Time behavior of a correlation peak. An asymmetric correlation peak $s(\tau)$ is shown—the same components exist for $\mathrm{tcp}(\tau)$. The horizontal scale is exaggerated. The pulse width (PW) could be $\lesssim$0.1 ps. Generally there could be fast (<PW), medium (1–10 PW), and slow (up to 1–3 ns) relaxation components. The medium component is not shown. The fast component (shaded) consists of incoherent (in) and coherent artifact (CA) components. The slow component causes the shoulder height Λ. The slow component amplitude is 50% at $\tau=0$. The repetition period (P), typically ~10 ns, is assumed much longer than the slow relaxation so that $s(P)\approx s(\infty)$. For an asymmetric correlation of a pulse train, negative delays greater than the pulse width are equivalent to positive delays of P. This is used to experimentally determine the baseline of $s(\tau)$ and hence $\mathrm{tcp}(\tau)$.

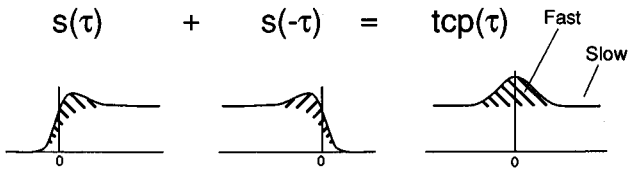

FIG. 4. Relation of asymmetric $s(\tau)$, and symmetric tcp(τ) correlation peaks. One could calculate tcp(τ)=$s(\tau)+s(-\tau)$. However, we recommend tcp(τ) be measured instead, since $\tau=0$ is then not required to accurately measure the shape due to the fast component (shaded). For $s(\tau)$, $\tau=0$ is uncertain experimentally since it is not at the maximum, and the presence of fast components confuse the step shape due to the slow components. The sole reason for measuring $s(\tau)$ is to provide the baseline $s(\infty)$, and hence tcp(∞).

$$^{\parallel}s_{\mathrm{in}}(0)=^{\parallel}s_{\mathrm{ca}}(0). \tag{26}$$

That is, the incoherent component is strictly 50% of the tcp(τ) or $s(\tau)$ in the $\parallel$ case, independent of Y values or the pulse shape assumed. This key point will help us determine the incoherent component height in the $\perp$ case, since for semiconductors $^{\perp}s_{\mathrm{in}}(0)\cong{}^{\parallel}s_{\mathrm{in}}(0)$.

By manipulation of Eq. (16) one can show that $\xi(w,-\tau)=\xi(w,\tau)$. Thus, the coherent artifact component is always symmetrical and centered at $\tau=0$, even for the asymmetrical correlations. By exploring Eq. (16), one finds that the CA shape does not change significantly with the material impulse response $A_{xyyx}(w)$. Instead, it depends most strongly on the laser pulse characteristics. Thus, the CA width cannot be used to learn material properties. However, the CA height can—it will yield T_θ.

Since TCP(τ)=$S(\tau)+S(-\tau)$, one may wonder why we recommend measuring both $^{\perp}$TCP(τ) and $^{\perp}S(\tau)$. Figure 4 illustrates that for the purpose of accurately determining the horizontal (delay-space) shape of the correlation due to the fast component, measuring TCP(τ) is superior, since it does not require knowledge of the $\tau=0$ position that the $S(\tau)+S(-\tau)$ operation requires. Accurate shapes are required to resolve the small increase in width of the TCP over the AC for fast relaxations. The zero delay position is hard to measure for $S(\tau)$ because the maximum of $S(\tau)$ does not occur at $\tau=0$, and because the presence of any fast components, including a coherent artifact, will confuse the side of the step due to the slow components. The only reason for measuring $S(\tau)$ is to determine the baseline for the TCP.

Although some of the data are recorded in the symmetric form, mathematically it is convenient to relate all the correlation components in their asymmetric forms. The heights and shapes in the two different forms are related by

$$\mathrm{tcp}(0)=2s(0), \tag{27}$$

$$\mathrm{tcp}(|\tau|>\text{several PW})=s(\tau>\text{several PW}). \tag{28a}$$

The region $\tau>$(several PW) is called the ''shoulder'' of the pulse. Also useful is

$$s(\tau>\text{several PW})\cong 2s(0) \tag{28b}$$

for slow relaxation components only.

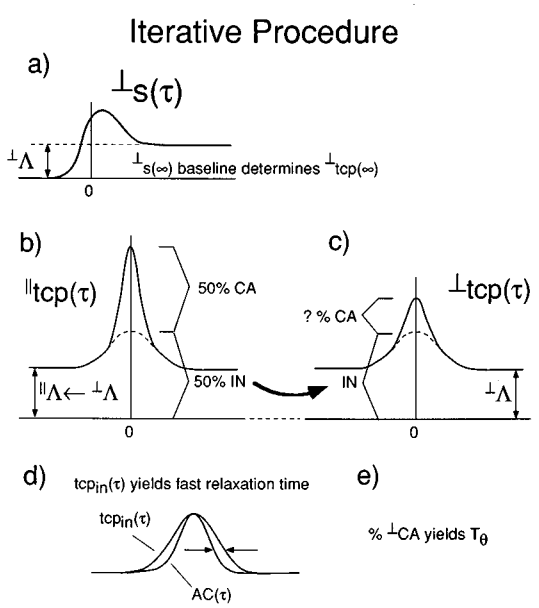

FIG. 5. The method for separating the coherent artifact (CA) from the incoherent (IN) portion. Both $\parallel$ and $\perp$ correlation peaks contain coherent and incoherent components, but in different ratios. (a) $^{\perp}s(\tau)$ shoulder height ($^{\perp}\Lambda$) provides the baseline for $^{\perp}$tcp(τ) and $^{\parallel}$tcp(τ). (b) The fraction of $\parallel$ incoherent component is strictly 50%. This yields the $\perp$ incoherent amplitude. (c) Subtraction from the total $\perp$ amplitude yields $^{\perp}$CA amplitude. The CA shape is independently determined. Deducting its shape from $^{\perp}$tcp(τ) yields the incoherent portion $\mathrm{tcp}_{\mathrm{in}}(\tau)$. (d) The width of the upper portion of $\mathrm{tcp}_{\mathrm{in}}(\tau)$ compared with AC(τ) yields the fast relaxation. (e) The height of CA yields T_θ. This whole procedure is iterated because the comparisons (a)–(e) depend on relaxation times, T_θ, AC width, CA width, and Y values to various degrees. The latter three quantities can be independently determined or presumed. The data are initially normalized so that TCP(∞)=1 and $S(\infty)=0.5$.

IV. ESSENCE OF METHOD

We seek the fraction of $^{\perp}$tcp(τ) which is the coherent artifact. The key feature of our technique is that we measure both the $\parallel$ and $\perp$ correlation cases. Fundamentally, this leads to a determination of the CA because both cases contain the CA, but in different ratios.

Figure 5 illustrates the method, which is fundamentally iterative because the steps depend to various degrees on T_θ and $G(t)$, which initially are unknown. The dependence is particularly strong if T_θ is comparable to PW.

The data are first normalized so that TCP(∞)=1 and $S(\infty)=0.5$. $^{\perp}s(\tau)$ is measured only for the purpose of determining its step height $^{\perp}\Lambda$ [Fig. 5(a)]. This yields the baseline for $^{\perp}$tcp directly, and for $^{\parallel}$tcp after considering Y values and T_θ. With the baselines established, exactly half the height of $^{\parallel}$tcp(0) is the incoherent portion [Fig. 5(b)]. $^{\parallel}\mathrm{tcp}_{\mathrm{in}}(0)$ is then used to find $^{\perp}\mathrm{tcp}_{\mathrm{in}}(0)$. For example, for semiconductors $^{\perp}\mathrm{tcp}_{\mathrm{in}}(0)\cong{}^{\parallel}\mathrm{tcp}_{\mathrm{in}}(0)$. Subtracting $^{\perp}\mathrm{tcp}_{\mathrm{in}}(0)$ from the total height of $^{\perp}$tcp(0) yields the height of the $\perp$ CA [Fig. 5(c)]. We suppose the CA shape is already known. Then scaling it by its height, we can subtract the CA shape from $^{\perp}$tcp(τ) to obtain $^{\perp}\mathrm{tcp}_{\mathrm{in}}(\tau)$.

A. Fitting for T_θ and $G(t)$

After obtaining $^{\perp}\mathrm{tcp}_{\mathrm{in}}(\tau)$ and $^{\perp}\mathrm{tcp}_{\mathrm{ca}}(\tau)$, we can fit for $G(t)$ and T_θ. By Eq. (13) we have

$$^{\perp}\mathrm{tcp}_{\mathrm{in}}(\tau)=\int_0^{\infty} dw A_{xxyy}(w)[\mathrm{AC}(\tau-w)+\mathrm{AC}(\tau+w)]. \tag{29}$$

This is a convolution of $\mathrm{AC}(t)$ with an unknown impulse response. The AC is measured experimentally. Any increase of the width of $\mathrm{tcp}_{\mathrm{in}}(\tau)$ over $\mathrm{AC}(\tau)$ will be due to relaxation processes [Fig. 5(d)]. These can be approximately found by evaluating Eq. (29) for an assumed $A(w)$ and comparing calculated and measured $\mathrm{tcp}_{\mathrm{in}}(\tau)$. (Approximately, since deconvolution is not a determinate process.) Relaxation components having widely disparate decay times will be more reliably identified than components of similar decays. Reference 20 discusses the use of linear predictive least-squares fitting to this kind of data.

Once $A_{xxyy}(t)$ is found, it can be related to $G(t)$. For the case of GaAs, $G(t)\approx A_{xxyy}(t)$ because $T_\theta<\mathrm{PW}$ and $Y_{xx}^2\approx Y_{xxyy}$.

Fitting the theory to the $^{\perp}$CA height yields T_θ. If $T_\theta\ll\mathrm{PW}$, the $^{\perp}$CA height grows linearly with T_θ/PW. The value of T_θ is interesting physics in itself.

B. The CA shape

The CA shape can be measured by the TCP of a dye such as Nile blue in ethylene glycol. Because $T_\theta\gg\mathrm{PW}$ for dyes when PW$\sim$0.1 ps, the coherent artifact can dominate the portion of the TCP resting above the slow component shoulders. This was shown to be the case for this dye.[21,22]

If the laser pulse is transform limited, the AC can be used to simulate the CA shape. The CA will never be wider than the AC, and will only be narrower if the pulse is chirped.

V. EVALUATION FOR GAUSSIAN PULSE

To facilitate investigating the behavior of the various correlation components, we model the pulse as Gaussian and $G(t)$ as a sum of exponential decays. This produces analytical expressions in the evaluation of Eqs. (11)–(19). Second, the Gaussian is a reasonable approximation to pulses obtained from some lasers.

A Gaussian $E_a(t)$ will produce Gaussian intensity envelope and Gaussian autocorrelations. Since often the pulse autocorrelation is the most convenient measurement of the pulse width, let PW represent the autocorrelation full width at half-maximum (FWHM). Then we have

$$E_a(t)=\exp(-t^2/a^2), \tag{30}$$

$$I(t)=\exp(-2t^2/a^2), \tag{31}$$

$$AC(\tau)=\int_{-\infty}^{\infty} dt I(t)I(t+\tau)=\Omega\ \exp(-\tau^2/a^2), \tag{32}$$

where

$$a\equiv PW/\sqrt{2\ln 2} \tag{33}$$

is the half-width at $\exp(-1)$ height, and

$$\Omega\equiv\sqrt{\pi}/2 \tag{34}$$

is a frequently used constant.

Let $G(t)$ be a sum of exponential decays of time constants T_i weighted by amplitudes α_i:

$$G(t)=\sum_i\ \alpha_i\ \exp(-t/T_i) \tag{35}$$

with $\Sigma_i\alpha_i=1$ so that $G(0)=1$. The exponential representation is convenient because it allows us to analytically combine the population relaxations with the dephasing relaxation, which was presumed to decay exponentially in Eq. (3).

Combining Eqs. (3), (11), (30), and (35) we have for either DI

$$^{\perp}\mathrm{DI}=^{\parallel}\mathrm{DI}=a\Omega\int_0^{\infty} dw\ \exp(-w^2/a^2)A_{xxxx}(w) \tag{36}$$

$$=a\Omega\int_0^{\infty} dw\ \exp(-w^2/a^2)[\exp(-w/T_\theta)$$

$$\times(Y_{xxxx}-Y_{xx}^2)+Y_{xx}^2]\sum_i\ \alpha_i\ \exp(-w/T_i) \tag{37}$$

$$=a^2\Omega\sum_i\ \alpha_i\{[Y_{xxxx}-Y_{xx}^2]U(T_i\oplus T_\theta,0)$$

$$+[Y_{xx}^2]U(T_i,0)\}. \tag{38}$$

The operator $\oplus$ means "sum as rates":

$$T_a\oplus T_b\equiv(T_a^{-1}+T_b^{-1})^{-1} \tag{39}$$

so that, just as resistors in parallel, the smaller value will control the final value. The function $U(T,\tau)$ is defined

$$U(T,\tau)\equiv\int_0^{\infty} dw\ \exp\{-(w-\tau)^2/a^2\}\exp\{-w/T\}, \tag{40}$$

$$U(T,\tau)=\Omega\ \exp[-(\tau/T)]\exp[(a/2T)^2]$$

$$\times\mathrm{erfc}[(a/2T)-\tau/a]. \tag{41}$$

The other correlation components are evaluated similarly:

$$^{\perp}s_{\mathrm{in}}(\tau)=a^2\Omega\sum_i\ \alpha_i\{[Y_{xxyy}-Y_{xx}^2]U(T_i\oplus T_\theta,\tau)$$

$$+[Y_{xx}^2]U(T_i,\tau)\}, \tag{42}$$

$$^{\perp}s_{\mathrm{ca}}(\tau)=a^2\Omega\ \exp\{-\tau^2/a^2\}\sum_i\ \alpha_i\{[Y_{xyyx}]U(T_i\oplus T_\theta,0)\}, \tag{43}$$

$$^{\parallel}s_{\mathrm{in}}(\tau)=a^2\Omega\sum_i\ \alpha_i\{[Y_{xxxx}-Y_{xx}^2]U(T_i\oplus T_\theta,\tau)$$

$$+[Y_{xx}^2]U(T_i,\tau)\}, \tag{44}$$

$$^{\parallel}s_{\mathrm{ca}}(\tau)=a^2\Omega\ \exp\{-\tau^2/a^2\}\sum_i\ \alpha_i\{[Y_{xxxx}-Y_{xx}^2]$$

$$\times U(T_i\oplus T_\theta,0)+[Y_{xx}^2]U(T_i,0)\}. \tag{45}$$

Again, we note $^{\parallel}s_{\mathrm{ca}}(0)=\ ^{\parallel}s_{\mathrm{in}}(0)$.

The function $U(T,\tau)$ has the behavior illustrated in Fig. 6. We are interested in the heights at $\tau=0$, by which we compare the correlation components. For $T/a\ll 1$

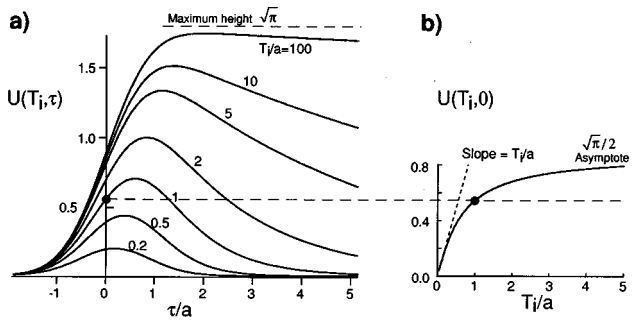

FIG. 6. The function $U(T_i,\tau)$ is the convolution of the Gaussian autocorrelation AC(τ) with exponential decay of relaxation time T_i. (a) vs delay τ for several relaxation times. For short relaxation times the convolution is an approximately symmetrical peak whose height grows linearly with T_i/a (b). For slow relaxation times the convolution is steplike, with maximum height $\sqrt{\pi}$.

$U(T,0)\rightarrow T/a$, and for $T\rightarrow\infty$, $U(T,0)\rightarrow\Omega$. Thus those relaxation processes that are faster than the pulse width will produce small amplitude correlation components that grow linearly with relaxation time. For relaxations much slower than the pulse width, the component will contribute to the shelflike nature of the $s(\tau)$ correlation. Since $\Sigma\ G(t)=1$, the total shoulder height that includes all components will never exceed $\sqrt{\pi/2}$ measured at $\tau=0$, or $\sqrt{\pi}$ measured many pulse widths away.

VI. ANALYSIS FOR A TWO-COMPONENT SYSTEM

To illustrate the qualitative behavior of the correlation components let us examine a system having only disparate fast and slow relaxation times T_f and T_s, respectively, where $T_f\ll a\ll T_s$ and having weighting $\alpha_f\approx\alpha_s$ where $\alpha_f+\alpha_s=1$. Let T_f be fast enough compared to the pulse width that we can approximate $U(T_f,0)\rightarrow T_f/a$, and T_s slow enough that we can approximate $U(T_s,0)\rightarrow\Omega$.

Equation (42) evaluated at $\tau=0$ is

$$
\begin{aligned}
{}^{\perp}s_{\mathrm{in}}(0)/a^2\Omega=&\alpha_f Y_{xx}^2 U(T_f,0)+\alpha_f[Y_{xxyy}-Y_{xx}^2]\\
&\times U(T_f\oplus T_\theta,0)+\alpha_s[Y_{xx}^2]U(T_s,0)\\
&+\alpha_s[Y_{xxyy}-Y_{xx}^2]U(T_s\oplus T_\theta,0). \qquad (46)
\end{aligned}
$$

Suppose we have the semiconductor case, where $T_\theta<T_f$. Then after using the approximations just described we have

$$
\begin{aligned}
{}^{\perp}s_{\mathrm{in}}(0)/a^2\Omega=&\alpha_f Y_{xx}^2(T_f/a)+[Y_{xxyy}-Y_{xx}^2](T_\theta/a)\\
&+\alpha_s[Y_{xx}^2]\Omega, \qquad (47)
\end{aligned}
$$

where we used $\alpha_f+\alpha_s=1$. We break this expression into fast and slow components, ${}^{\mathrm{fast}\perp}s_{\mathrm{in}}(0)$ and ${}^{\mathrm{slow}\perp}s_{\mathrm{in}}(0)$, because the slow components are associated with a shoulder for $\tau>a$ having twice the $\tau=0$ height, whereas the fast components are not. The last term of Eq. (47) is the slow component. We can ignore the constant $a^2\Omega$, because it appears for every component.

The expression for the coherent artifact can be similarly evaluated. Although the coherent artifact could be called a fast component (since it produces no shoulder), we distinguish it from the fast incoherent component. There is no slow coherent component.

TABLE II. Dye molecule case. Heights of fast and slow incoherent, and coherent artifact components at $\tau=0$ for $s(\tau)$ when $T_f\ll a\ll T_\theta<T_s<P$ and using the limiting approximations for $U(T,0)$. Each entry should be multiplied by $a\Omega^2$. Note that the $\|$ and $\perp$ cases are in the ratio $Y_{xxxx}/Y_{xxyy}=3$ for every component.

	$\|$ case	$\perp$ case
Fast (fast incoherent)	$\alpha_f(T_f/a)\ Y_{xxxx}$	$\alpha_f(T_f/a)\ Y_{xxyy}$
Slow	$\alpha_s\Omega\ Y_{xxxx}$	$\alpha_s\Omega\ Y_{xxyy}$
CA (fast coherent)	Fast+slow	Fast+slow

Analogous to Eq. (47), we evaluate all the $\tau=0$ component heights for the $\perp$ and $\|$ cases and list them in Tables II and III, for the semiconductor and dye molecule cases. In the semiconductor case $T_\theta<T_f\ll a\ll T_s<P$, and the dye molecule case $T_f\ll a\ll T_\theta<T_s<P$.

Note that in the dye molecule case, the $\|$ and $\perp$ cases are in the ratio $Y_{xxxx}/Y_{xxyy}=3$ (Table I) for every component, incoherent and coherent [Fig. 7(a)]. The CA is 50% of the total correlation, for both $\|$ and $\perp$ cases. This can create TCPs where the fast part consists almost entirely of CA, if $T_f\ll a$ or if $\alpha_f\ll\alpha_s$.

For the semiconductor case, note that since $Y_{xxxx}\approx Y_{xxyy}$ (Table I) and T_θ/a is assumed small, the fast and slow incoherent components are, or nearly are the same between the $\|$ and $\perp$ cases [Fig. 7(b)]. Thus the baseline of ${}^{\perp}\mathrm{tcp}(\tau)$ found from the shoulder height Λ of ${}^{\perp}s(\tau)$ applies almost directly to ${}^{\|}\mathrm{tcp}(\tau)$ as well. That is, the incoherent portions of ${}^{\perp}\mathrm{tcp}$ and ${}^{\|}\mathrm{tcp}$ are nearly the same [Figs. 5(b) and 5(c)]. This is particularly true of the slow component.

We can derive a simple estimate for the fraction of coherent artifacts based on two easily measured parameters R and Q (Fig. 8). R is the ratio of the fast portion of tcp(τ) heights, that is, the portion that lies above the shoulder, between the $\|$ and $\perp$ cases. Q describes the height of $s(0)$ compared to its shoulder.

$$
R\equiv\frac{{}^{\|}\mathrm{tcp}(0)-{}^{\|}\mathrm{tcp}(\mathrm{shoulder})}{{}^{\perp}\mathrm{tcp}(0)-{}^{\perp}\mathrm{tcp}(\mathrm{shoulder})}, \qquad (48)
$$

$$
Q\equiv\frac{{}^{\perp}\mathrm{sig}(0)}{{}^{\perp}\mathrm{sig}(\mathrm{shoulder})}. \qquad (49)
$$

The ''shoulder'' is a delay longer than the autocorrelation or fast relaxation time, but slower than the slow relaxation time.

TABLE III. Semiconductor case. Heights of fast and slow incoherent, and coherent artifact components at $\tau=0$ for $s(\tau)$ when $T_\theta<T_f\ll a\ll T_s<P$ and using the limiting approximations for $U(T,0)$. Each entry should be multiplied by $a\Omega^2$. Note that since $Y_{xxxx}\approx Y_{xxyy}$ and T_θ/a is small for the semiconductor, the fast and slow incoherent components are, or nearly are the same between the $\|$ and $\perp$ cases.

	$\|$ case	$\perp$ case
Fast (fast incoherent)	$\alpha_f(T_f/a)\ Y_{xx}^2$ $+\alpha_f(T_\theta/a)[Y_{xxxx}-Y_{xx}^2]$	$\alpha_f(T_f/a)\ Y_{xx}^2$ $+\alpha_f(T_\theta/a)[Y_{xxyy}-Y_{xx}^2]$
Slow	$\alpha_s\Omega\ Y_{xx}^2$	$\alpha_s\Omega\ Y_{xx}^2$
CA (fast coherent)	Fast+slow	$Y_{xyyx}\ (T_\theta/a)$

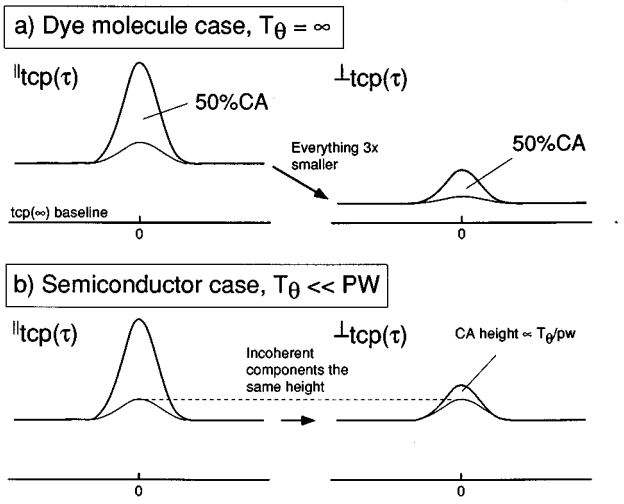

FIG. 7. Example cases for two extremes of T_θ/PW. We do not show any medium time-scale relaxation, only fast and slow. (a) For a dye molecule $T_\theta \gg$PW. Because of Eq. (3), the coherent artifact (CA) height equals the incoherent portions in both $\perp$ and $\parallel$ cases. However, the overall size is $Y_{xxxx}/Y_{xxyy}=3$ times different between the two cases. (b) For a semiconductor we could have $T_\theta \ll$PW. By Eq. (3), the incoherent terms have similar magnitude in $\parallel$ and $\perp$ cases. However, the coherent terms are different. For the $\parallel$ case, it is as large as the incoherent term. For the $\perp$ case it is much smaller and grows as T_θ/PW.

We seek the fractional height of the CA, as a fraction of the portion of the measured tcp height lying above the shoulder. Define this fraction as "frac":

$$\text{frac} \equiv \frac{^{\perp}\text{tcp}_{\text{ca}}(0)}{^{\perp}\text{tcp}(0) - ^{\perp}\text{tcp}(\text{shoulder})} = \frac{^{\perp}s_{\text{ca}}(0)}{^{\perp}s_{\text{ca}}(0) + ^{\perp \text{fast}}s_{\text{in}}(0)}. \tag{50}$$

Since we are primarily interested in the semiconductor case, we will assume that the slow components have the same height between the $\perp$ and $\parallel$ cases. Using the heights listed in Table III for the semiconductor, and noting that the slow component is twice as high at the shoulder as at $\tau=0$, we get after some algebra,

$$\text{frac} = 1 - \frac{R}{2\beta} + \frac{1}{2\beta(2Q-1)}. \tag{51}$$

β is the ratio between the fast component heights

$$\beta \equiv {}^{\parallel \text{fast}}s_{\text{in}}(0)/{}^{\perp \text{fast}}s_{\text{in}}(0) \approx 1, \tag{52}$$

for a semiconductor.

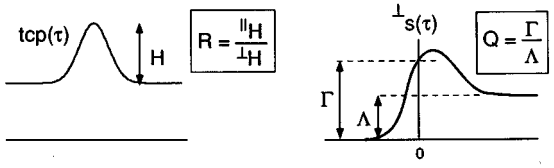

FIG. 8. Definition of R and Q. H is the height of tcp(τ) above its immediate shoulders, measured between $\perp$ and $\parallel$ configurations. The ratio is R. Q describes how high $^{\perp}s(0)$ is relative to the shoulder height. Note, the peak of $^{\perp}s(\tau)$ is not the same as $^{\perp}s(0)$.

Inspecting the fast components of Table III, we see for semiconductors $\beta \approx 1$ if $T_\theta < T_f$, since $[Y_{xxxx} - Y_{xx}^2]$ and $[Y_{xxyy} - Y_{xx}^2]$ are several times smaller than $(Y_{xx})^2$, according to Table I.

Note that the R, Q, and frac definitions are very practical, since they refer to the portion of the TCP(τ) or $S(\tau)$ lying above the shoulder, which is the experimentally observed background level.

We remind the reader again that Eq. (51) is not appropriate for the dye case, because of the assumption that the slow components have the same heights between the $\perp$ and $\parallel$ cases. Furthermore, this result is not intended to be a final result, but the initial guess of an iterative procedure. This is because it was assumed there were no medium scale decay components and $a \ll T_s$, so that the TCP shoulder was level and well defined. In reality, the presence of decays comparable to the pulse width would confuse Eq. (51).

VII. DISCUSSION

A. Small signal regime

Equation (2) presumes the small signal regime, since for arbitrarily large optical intensities Eq. (2) predicts arbitrarily large induced polarization, when in reality the polarization must be limited. The integral in Eq. (2) in essence expresses the number of carriers excited from the valence to conduction band, in the semiconductor idiom, or the number of excited dye molecules. Obviously this number is limited by the number of carriers or number of dye molecules in the sample.

Given that we are in the small signal regime, this implies that if the relaxation rates are carrier density independent then the physical thickness of the sample or the distribution of absorptivity with depth is immaterial. This is because the carriers are not competing with each other for a limited number of conduction band sites. However, some semiconductor scattering processes, such as carrier–carrier scattering, are carrier density dependent.[4] Thus, to minimize the variation of excited carrier density with depth, the sample should be optically thin.

An optically thin sample can be in either the large or small signal regime, depending on the number of photons in the pulse relative to the number of absorbing centers integrated through the sample depth. This should be confirmed experimentally by measuring the fractional TCP height versus laser power. For low powers, the relationship should be a power law with a slope near unity. As the power passes a threshold, the slope will begin to decrease indicating a change from the small to large signal regime. The large signal regime should be avoided even for carrier density independent scattering rates, since it will limit the fractional height of the TCP and therefore make it appear broader than this theory predicts, yielding erroneous relaxation times.

B. Procedure overview

To separate the various correlation components and fit for relaxation and dephasing times, we recommend the iterative procedure outlined in Fig. 5. By comparing calculated and experimental signals between $\perp$ and $\parallel$ cases, the coherent

artifact height can be found. Once separated, fitting to the shapes and heights of the component correlations yields T_θ and $G(t)$. These both manifest interesting physics.

The correlation component heights and shapes would be calculated either using the Gaussian model Eqs. (42)–(45), or the exact expressions Eqs. (11)–(19) calculated numerically using the experimentally measured autocorrelation and presumed $G(t)$ and T_θ. For the numerical evaluation, $G(t)$ could be nonexponential. The equations can easily be modified for unequal intensities between the two arms. Initial guesses for T_θ and $G(t)$ could be obtained with the help of Eq. (51) for semiconductor samples. Knowledge of the Y coefficients for the particular sample being studied is required. These can be calculated from Refs. 4 and 17 using the semiconductor band structure. These Y coefficients do not require knowledge of the sample dynamics.

ACKNOWLEDGMENTS

This work was performed at Lawrence Livermore National Laboratory under the auspices of the U.S. Department of Energy under Contract No. W-7405-ENG-48.

[1] J. E. Bair, D. Cohen, J. P. Krusius, and C. R. Pollock, Phys. Rev. B **50**, 4355 (1994).
[2] A. J. Taylor, D. J. Erskine, and C. L. Tang, Appl. Phys. Lett. **43**, 989 (1983).
[3] C. L. Tang and D. J. Erskine, Phys. Rev. Lett. **51**, 840 (1983).
[4] A. J. Taylor, D. J. Erskine, and C. L. Tang, J. Opt. Soc. Am. B **2**, 663 (1985). Equation (2) of this reference should read $A_{ijkl}(w)$, not $A_{ijkl}(t-w)$.
[5] D. J. Erskine, A. J. Taylor, and C. L. Tang, Appl. Phys. Lett. **45**, 54 (1984).
[6] D. J. Erskine, A. J. Taylor, and C. L. Tang, Appl. Phys. Lett. **45**, 1209 (1984).
[7] C. L. Tang, F. W. Wise, and I. A. Walmesly, Rev. Phys. Appl. **22**, 1695 (1987).
[8] M. J. Rosker, F. W. Wise, and C. L. Tang, Appl. Phys. Lett. **49**, 1726 (1986).
[9] F. Wise, I. A. Walmsley, and C. L. Tang, Appl. Phys. Lett. **51**, 605 (1987).
[10] D. J. Erskine, A. J. Taylor, and C. L. Tang, J. Chem. Phys. **80**, 5338 (1984).
[11] F. W. Wise, M. J. Rosker, and C. L. Tang, J. Chem. Phys. **86**, 2827 (1987).
[12] M. Lindberg, Y. Z. Hu, R. Binder, and S. W. Koch, Phys. Rev. B **50**, 18060 (1994).
[13] D. S. Chemla, Solid State Commun. **92**, 37 (1994).
[14] R. Binder, D. Scott, A. E. Paul, M. Lindberg, K. Henneberger, and S. W. Koch, Phys. Rev. B **45**, 1107 (1992).
[15] R. Scholz and A. Stahl, Phys. Status Solidi B **173**, 199 (1992).
[16] M. Bonitz, D. Kremp, D. C. Scott, R. Binder, and W. D. Kraeft (unpublished).
[17] B. S. Wherrett, A. L. Smirl, and T. F. Boggess, IEEE J. Quantum Electron. **QE-19** (4), 680 (1983).
[18] T. Elsaesser, J. Shah, L. Rota, and P. Lugli, Phys. Rev. Lett. **66**, 1757 (1991).
[19] N. Bloembergen, *Nonlinear Optics* (Benjamin, Reading, MA, 1965).
[20] F. W. Wise, M. J. Rosker, G. L. Millhauser, and C. L. Tang, IEEE J. Quantum Electron. **QE-23**, 1116 (1987).
[21] A. J. Taylor, D. J. Erskine, and C. L. Tang, in *Proceedings of the IVth Workshop on Ultrafast Phenomena* (Springer, Berlin, 1984).
[22] T. F. Heinz, S. L. Palfrey, and K. B. Eisenthal, Opt. Lett. **9**, 359 (1984).